https://doi.org/10.5194/acp-2021-730
Preprint. Discussion started: 21 October 2021

Atmospheric Chemistry and Physics Discussions

The formation and mitigation of nitrate pollution: Comparison between urban and suburban environments

Suxia Yang[1,2], Bin Yuan[1,2*], Yuwen Peng[1,2], Shan Huang[1,2], Wei Chen[3], Weiwei Hu[3], Chenglei Pei[3,4,5,6], Jun Zhou[1,2], David D. Parrish[1], Wenjie Wang[7], Xianjun He[1,2], Chunlei Cheng[2,8], Xiaobing Li[1,2], Xiaoyun Yang[1,2], Yu Song[7], Haichao Wang[9], Jipeng Qi[1,2], Baolin Wang[10], Chen Wang[10], Chaomin Wang[1,2], Zelong Wang[1,2], Tiange Li[1,2], E Zheng[1,2], Sihang Wang[1,2], Caihong Wu[1,2], Mingfu Cai[1,2], Chenshuo Ye[7], Wei Song[3], Peng Cheng[7], Duohong Chen[6], Xinming Wang[3], Zhanyi Zhang[1,2], Xuemei Wang[1,2], Junyu Zheng[1,2], Min Shao[1,2*]

[1]Institute for Environmental and Climate Research, Jinan University, Guangzhou 511443, China

[2]Guangdong-Hongkong-Macau Joint Laboratory of Collaborative Innovation for Environmental Quality, Jinan University, Guangzhou 511443, China

[3]State Key Laboratory of Organic Geochemistry and Guangdong Key Laboratory of Environmental Protection and Resources Utilization, Guangzhou Institute of Geochemistry, Chinese Academy of Sciences, Guangzhou 510640, China

[4]CAS Center for Excellence in Deep Earth Science, Guangzhou, 510640, China

[5]University of Chinese Academy of Sciences, Beijing 100049, China

[6]Guangzhou Ecological and Environmental Monitoring Center of Guangdong Province, Guangzhou 510060, China

[7]State Joint Key Laboratory of Environmental Simulation and Pollution Control, College of Environmental Sciences and Engineering, Peking University, Beijing 100871, China

[8]Institute of Mass Spectrometry and Atmospheric Environment, Guangdong Provincial Engineering Research Center for on-line Source Apportionment System of Air Pollution, Jinan University, Guangzhou 510632, China

[9]School of Atmospheric Sciences, Sun Yat-Sen University, Guangzhou 510275, China

[10]School of Environmental Science and Engineering, Qilu University of Technology, Jinan 250353, China

Correspondence to: Bin Yuan (byuan@jnu.edu.cn) and Min Shao (mshao@pku.edu.cn)

https://doi.org/10.5194/acp-2021-730
Preprint. Discussion started: 21 October 2021

Atmospheric Chemistry and Physics Discussions

Abstract. Ambient nitrate has been of increasing concern in $PM_{2.5}$, while there are still large uncertainties in quantifying the formation of nitrate aerosol. The formation pathways of nitrate aerosol at an urban site and a suburban site in the Pearl River Delta (PRD) are investigated using an observation-constrained box model. Throughout the campaigns, aerosol pollution episodes were constantly accompanied with the increase of nitrate concentrations and fractions at both urban and suburban sites. The simulations demonstrate that chemical reactions in the daytime and at night both contributed significantly to formation of nitrate in the boundary layer at the two sites. However, nighttime reactions predominately occurred aloft in the residual layer at the urban site and downward transport from the residual layer in the morning are important source (53%) for surface nitrate at the urban site, whereas similar amounts of nitrate were produced in the nocturnal boundary layer and residual layer at the suburban site, which results in little downward transport of nitrate from the residual layer to the ground at the suburban site. We show that nitrate formation was in the volatile organic compounds (VOCs)-limited regime at the urban site, and in the transition regime at the suburban site, identical to the response of ozone at both sites. The reduction of VOCs emissions can be an efficient approach to mitigate nitrate in both urban and suburban areas through influencing hydroxyl radical (OH) and N_2O_5 production, which will also be beneficial for the synergistic control of regional ozone pollution. The results highlight that the relative importance of nitrate formation pathways can be site-specific, and the quantitative understanding of various pathways of nitrate formation will provide insights for developing nitrate mitigation strategies.

Keywords: nitrate, ozone, volatile organic compounds, N_2O_5, formation pathways, urban and suburban sites

https://doi.org/10.5194/acp-2021-730
Preprint. Discussion started: 21 October 2021


Atmospheric Chemistry and Physics Discussions

1 Introduction

Particulate nitrate is a substantial chemical component of fine particles, which plays a significant role in the acid deposition, visibility reduction, hygroscopic property, and radiative forcing (Li et al., 1993;Watson, 2002;Pathak et al., 2009;Xu and Penner, 2012;Zhang et al., 2017;Liu et al., 2020). Due to the larger emission reduction of SO_2 than NO_x since the implementation of the clean air actions in China, a considerable increase in the nitrate fractions in aerosols has been observed in haze periods in the northern China Plain (Wen et al., 2018;Li et al., 2018;Lu et al., 2013;Fu et al., 2020), southern China (Pathak et al., 2009;Pathak et al., 2011) and eastern China(Griffith et al., 2015;Tao et al., 2018;Yun et al., 2018b;Li et al., 2018), which indicates the growing significance of nitrate in the formation of haze events. In addition, the photolysis of particulate nitrate can increase the production of sulfate and nitrous acid (HONO), implying the importance of nitrate in the synergetic enhancement of the atmospheric oxidizing capability in haze events (Gen et al., 2019;Zhang et al., 2020;Ye et al., 2016;Ye et al., 2017). Hence, identifying and understanding the driving factors of nitrate formation are essential to establishment of optimized mitigation policies for fine particles.

Particulate nitrate is primarily produced through two processes: the photochemical reaction of hydroxyl radical (OH) and NO_2 during daytime (R1) and the heterogeneous uptake of N_2O_5 (R2–R5) during nighttime. The gaseous nitric acid (HNO_3) is produced by the reaction of OH and NO_2, and then reacts with ammonia (NH_3) to form particulate nitrate (Stelson and Seinfeld, 1982). The partitioning process of HNO_3 between the gas and particle phase is regulated by ambient temperature (T), relative humidity (RH), and the abundance of NH_3 (R7) (Mozurkewich, 1993;Xue et al., 2014a;Yun et al., 2018b). The heterogeneous uptake reaction of N_2O_5 is affected by the coefficient (γ) and the production yield of $ClNO_2$ (φ) (R5), which cannot be directly measured and are significantly impacted by the aerosol components and ambient RH (Bertram and Thornton, 2009;McDuffie et al., 2018). Thus, the nocturnal contribution to nitrate formation still has great uncertainty.

In addition, the heterogeneous uptake of N_2O_5 in the nocturnal boundary layer (NBL) is greatly disturbed in the presence of fresh NO emissions, which titrate the NO_3 radical within the stagnant boundary layer (Geyer and Stutz, 2004;Li et al., 2020;Chen et al., 2020). However, aircraft observations in California and Utah in the US have

https://doi.org/10.5194/acp-2021-730
Preprint. Discussion started: 21 October 2021

Atmospheric Chemistry and Physics Discussions

revealed that active uptake of N_2O_5 in the residual layer contributed a major portion of the near-surface nitrate accumulation during the morning transport from aloft (Prabhakar et al., 2017;McDuffie et al., 2019;Womack et al., 2019). Similarly, ground- and tower-based field observations also pointed out the important contribution of this pathway to the rapid increase of near-surface nitrate concentrations in Beijing, China (Wang et al., 2018a;Chen et al., 2020). However, under different atmospheric conditions, the relative importance of nitrate production varies significantly within the residual layer (McDuffie et al., 2019;Tang et al., 2021), giving widely varying relative contributions of the major chemical pathways to nitrate pollution among different sites (Wang et al., 2018a;Womack et al., 2019;Chen et al., 2020;Lin et al., 2020). A comprehensive understanding of the nitrate production in the residual layer is required to quantify the contributions of different formation pathways to nitrate pollution.

$$OH + NO_2 \xrightarrow{k_1} HNO_3(g) \quad \text{R1}$$

$$NO_2 + O_3 \xrightarrow{k_2} NO_3 + O_2 \quad \text{R2}$$

$$NO_3 + NO_2 \overset{k_3}{\leftrightarrow} N_2O_5 \quad \text{R3}$$

$$NO_3 + VOCs \rightarrow products \quad \text{R4}$$

$$N_2O_5 + (H_2O \text{ or } Cl^-) \xrightarrow{k_5} \varphi ClNO_2 + (2-\varphi)NO_3^-(p) \quad \text{R5}$$

$$ClNO_2 \xrightarrow{k_6} Cl\cdot + NO_2 \quad \text{R6}$$

$$HNO_3(g) + NH_3(g) \overset{k_7}{\leftrightarrow} NO_3^-(p) + NH_4^+(p) \quad \text{R7}$$

The nitrate production from the reaction of OH and NO_2 pathway during daytime is well-understood, and the control of NO_x emission is commonly considered as an effective strategy to reduce ambient nitrate. However, several studies reported that the efficiency of NO_x reduction in nitrate control is limited, and it may enhance nitrate production under some conditions (Womack et al., 2019;Dong et al., 2014;Hou et al., 2019). The study by Womack et al. (2019) showed that both nitrate and ozone were VOCs-limited in Salt Lake City, suggesting that VOCs control would effectively reduce nitrate. Similarly, modeling studies also found that the nitrate formation was more sensitive to the change in VOCs concentrations over the northern and eastern China (Dong et al., 2014;Lu et al., 2019;Fu et al., 2020). However, the sensitivity of nitrate production to both NO_x and VOCs in different regions should be comparatively evaluated, which could provide helpful implications in formulating effective control strategies for the mitigation of aerosol pollution.

https://doi.org/10.5194/acp-2021-730
Preprint. Discussion started: 21 October 2021

Atmospheric Chemistry and Physics Discussions

In recent years, the nitrate formation in haze episodes has been studied in northern China (Liu et al., 2015;Wang et al., 2017a;Wen et al., 2018;Fu et al., 2020;Chen et al., 2020), eastern China (Tao et al., 2016;Lin et al., 2020) and southern China (Qin et al., 2017;Tao et al., 2018;Yun et al., 2018b;Su et al., 2020), and the important contribution of the heterogeneous uptake of N_2O_5 in the nighttime has been discussed (Wang et al., 2017b;Yun et al., 2018b;Yun et al., 2018a;Chen et al., 2020). However, these ground-based observations rarely considered the potential contributions of reactive uptake of N_2O_5 aloft in the residual layer, which could be an important source of near-surface nitrate concentrations. In addition, few studies have comprehensively evaluated the relative influence of NO_x and VOCs reductions on nitrate production in different environments (Hou et al., 2019).

In this study, we present the results from the ground- and tower-based measurements in both urban and suburban areas in southern China. An observation-constrained box model was used to simulate the production rates of nitrate from different formation pathways, and to compare the effects of reducing NO_x and VOCs emissions in both urban and suburban areas. This work provides new insights into the synergetic mitigation of particle and ozone pollution, which can guide development of the most effective nitrate control strategies.

2 Method and data

2.1 Field observation

The ground-based field measurements were conducted at both an urban site in Guangzhou and a suburban site in Heshan. The tower-based measurements were conducted at an urban site in Guangzhou. The ground-based study in Guangzhou was carried out from late September to mid-November in 2018 at the Institute of Geochemistry (GIG), Chinese Academy of Sciences (23.1°N, 113.2°E), which is a typical urban site surrounded by a residential area and traffic avenues (Fig. 1). The instruments were deployed on the top of the 25-m building at GIG site. The ground-based measurement at the suburban site was performed from late September to mid-November in 2019 at the supersite of Heshan county (22.7°N, 112.9°E), which is approximately 50 km southwest to Foshan and 80 km southwest to Guangzhou, and is frequently influenced by anthropogenic emissions from upward Guangzhou-Foshan mega-city areas. The tower-based measurements in Guangzhou were conducted

https://doi.org/10.5194/acp-2021-730
Preprint. Discussion started: 21 October 2021


Atmospheric Chemistry and Physics Discussions

simultaneously at the ground and 448 m on the Canton Tower in Guangzhou, which is located approximately 5.7 km away from the GIG site (Fig. 1).

The chemical components of PM_1, trace gases, and non-methane hydrocarbons (NMHC) were both measured at the GIG and Heshan sites, whereas only trace gases (NO_x and O_3) and meteorological parameters were measured at the Canton Tower site. The non-refractory chemical compositions of PM_1 (NR-PM_1), including organics (Org), sulfate (SO_4^{2-}), nitrate (NO_3^-), ammonium (NH_4^+), and chloride (Cl^-) were measured using a high-resolution time-of-flight aerosol mass spectrometer (HR-ToF-AMS, Aerodyne Research Inc., US) (Hu et al., 2016;Chen et al., 2021). Black carbon (BC) was measured using an aethalometer (AE33, Magee Scientific Co., US). Particle number size distribution was measured using a scanning mobility particle sizer with an aerodynamic diameter ranging from 10 to 650 nm (SMPS, TSI, US) and aerosol particle sizer ranging from 500 nm to 20 μm (APS, TSI, US).

HNO_3, N_2O_5, and $ClNO_2$ were measured using iodide-time-of-flight chemical ionization mass spectrometry (Iodide-TOF-CIMS, Aerodyne Research Inc., US) (Wang et al., 2020b;Ye et al., 2021). The non-methane hydrocarbons (NMHC) were measured using online GC-MS-FID (Wuhan Tianhong Co., Ltd, China) (Yuan et al., 2012) (Table S2). The concentrations of oxygenated VOCs (OVOCs), including formaldehyde (HCHO) and acetaldehyde (CH_3CHO), were measured via a high-resolution proton transfer reaction time-of-flight mass spectrometry (PTR-ToF-MS, Ionicon Analytik, Austria) (Wang et al., 2020a;Wu et al., 2020). HONO was detected using a long path absorption photometer (LOPAP) at the GIG site (Yu et al., 2021), and was measured by the gas and aerosol collector (GAC) instrument at the Heshan site (Dong et al., 2012;Yang et al., 2014). NH_3 was also measured by two sets of instruments: a cavity ring-down spectroscopy (CRDS, Picarro, US) was used at the GIG site and the GAC instrument was used at the Heshan site. Details on the limit of detection and accuracy of the instruments are presented in Table S1.

In addition, trace gases (O_3 (49i), NO_x (42i), CO (48i) and SO_2 (43i)) (Thermo Scientific, US) and meteorological parameters (i.e., wind speed (WS), wind direction (WD), temperature (*T*), relative humidity (RH) and pressure (*P*)) (Vantage Pro 2, Davis Instruments Co. , US) were simultaneously measured during these campaigns. The photolysis frequencies of O_3, NO_2, HCHO, and HONO (PFS-100, Focused Photonics Inc., China) were also measured during the campaign.

https://doi.org/10.5194/acp-2021-730
Preprint. Discussion started: 21 October 2021

Atmospheric Chemistry and Physics Discussions

Considering the integrity and temporal coverage of the measurements, we mainly focus on the investigated periods from October 7 to 29, 2018, at the GIG site and from October 16 to November 16, 2019, at the Heshan site.

2.2 Model description

A zero-dimensional observation-based box model (F0AM) (Wolfe et al., 2016) was used to simulate the production of nitrate in this study. The F0AM box model uses a subset of the Master Chemical Mechanism (MCM) v3.3.1, which explicitly describe chemical reactions of VOCs, RO_x radicals (including OH, HO_2 and RO_2), ozone and nitrate.

In this study, the box model was constrained by observations of NMHCs, HCHO, CH_3CHO, NO, CO, CH_4, HONO, and meteorological parameters (i.e., photolysis rates, RH, *T* and *P*) measured at the GIG and Heshan sites. To investigate the convection of nitrate between the residual layer and the surface, the box model was split into two boxes at night (from 17:00 to 6:00 of the following morning) to separately represent the nocturnal boundary layer and the residual layer, respectively (Womack et al. (2019) (Fig. S1).

The simulation of the residual layer at the GIG site was constrained by the observation data from 488 m at the Canton Tower, while the simulation of the residual layer at the Heshan site was freely evolved from sunset time using the ground observation data of Heshan. The detailed model settings are described in Text S1, and the agreement between the observation data and simulations at the GIG and Canton Tower sites supports the use of similar simulation of the residual layer at the Heshan site. The model was operated in a time-dependent mode with a 5-min resolution. It was run for a 72-hour spin-up time to build steady-state concentrations for secondary pollutants that were not constrained during simulation. To prevent the build-up of secondary species to unreasonable levels, an additional physical dilution process with a lifetime of 24 h was applied in the model. The background concentrations for ozone and CH_4 were set as 30 ppb and 1.8 ppm, respectively (Wang et al., 2011).

The nocturnal production of nitrate from N_2O_5 hydrolysis and the subsequent reactions (R5 and R6) are added to the box model. The reaction rates of R5 and R6 are expressed as Eqs.1 and 2, respectively:

$$k_5 = \frac{\omega 1 * \gamma * Sa}{4} \quad \text{(Eq.1)}$$

https://doi.org/10.5194/acp-2021-730
Preprint. Discussion started: 21 October 2021

Atmospheric Chemistry and Physics Discussions

$k_6 = J_{ClNO_2}$ (Eq.2)

where ω_1 is the average molecular speed of N_2O_5, γ is the uptake coefficient of N_2O_5 and φ is the production yield of $ClNO_2$ in R5. γ and φ are calculated using the new observation-based empirical parameterization method from Yu et al. (2020), where the impacts of nitrate, chloride, and aerosol liquid water content (ALWC) were evaluated to better represent the observed γ. The average values of γ were 0.018±0.01 and 0.019±0.01 at the GIG and Heshan sites, respectively, which were comparable with those observed data at the Heshan site in 2017. The φ used in this study were 0.18±0.15 and 0.20±0.23 at the GIG and Heshan sites, which were slightly lower than the observed data at the Heshan site (0.31 ± 0.27) (Yu et al., 2020). The chemical compositions of fine particles were not measured at the Canton Tower site, thus values of γ and φ in the residual layer were assigned equal to those of the nocturnal boundary layer. This may lead to negative deviations for γ and positive deviations for φ in the residual layer, as higher RH and lower $PM_{2.5}$ concentrations were observed in the residual layer (as shown in Fig.S4). The dry aerosol surface area concentration (S_a) was calculated from the particle number size distribution and calibrated to the actual atmospheric S_a using the RH-dependent hygroscopic growth factor (f(RH)). f(RH) was calculated using the aerosol compositions measured by AMS and estimated liquid water by thermodynamic model of ISORROPIA, according to the study conducted by McDuffie et al. (2018). The photolysis frequency of $ClNO_2$, denoted as k_6, was scaled from measured NO_2 photolysis frequencies divided by a factor of 30 (Riedel et al., 2014).

The equilibrium coefficient between HNO_3 and particulate nitrate is incorporated into the box model as a pseudo-first-order reaction (Eqs.3 and 4) through the equilibrium absorption partitioning theory (Yuan et al., 2016;Jacob, 2000):

$$HNO_3\ (g) \underset{k_{8b}}{\overset{k_{8f}}{\Leftrightarrow}} NO_3^-\ (p) \quad \text{R8}$$

$$k_{8f} = \left(\frac{R_a}{D_g} + \frac{4}{\omega * \alpha}\right)^{-1} * S_a \quad \text{(Eq.3)}$$

$$k_{8b} = \left(\frac{R_a}{D_g} + \frac{4}{\omega * \alpha}\right)^{-1} \frac{S_a}{K_{eq}} \quad \text{(Eq.4)}$$

where R_a is the radius of nitrate particles, D_g is the gas-phase molecular diffusion coefficient ($m^2\ s^{-1}$), ω is the mean molecular speed of HNO_3, α is the mass accommodation coefficient of HNO_3, and K_{eq} represents the equilibrium constant of

https://doi.org/10.5194/acp-2021-730
Preprint. Discussion started: 21 October 2021


Atmospheric Chemistry and Physics Discussions

HNO_3 and nitrate. These coefficients are the same as those in the chemical aqueous-phase radical mechanism (CAPRAM) (Ervens et al., 2003;Wen et al., 2015).

The empirical kinetic modeling approach (EKMA) is used here to identify the sensitivity of ozone and nitrate to the variations of NO_x and VOCs. The observed diurnal average conditions are used as the input for the base simulation. Sensitivity tests are conducted by increasing and decreasing initial anthropogenic VOCs (AVOCs) and NO_x concentrations by a ratio ranging from 0.1 to 2.0 with 20 equal-distance steps without changing other parameters in the model (Tan et al., 2018;Lyu et al., 2019;Womack et al., 2019). The maximum concentration of ozone and nitrate in each scenario are plotted to generate the contour plots of the respective isopleths. Reducing biogenic VOCs (BVOCs) such as isoprene is impractical, so they are not scaled with AVOCs concentrations in the simulations.

Constraining N_2O_5 concentrations with the change in NO_x ratio arbitrarily during the isopleth simulations is meaningless. Thus, we set the simulation of base case without N_2O_5 constrained. To evaluate the results of the base case, we compare the simulated nitrate with and without the N_2O_5 constrained in Fig. S2. The base case simulation was comparable to the results without N_2O_5 constrained. The simulated nitrate with N_2O_5 constrained during October 9 to 10, 2018 was observed to be higher compared to both the observations and base case simulation at the GIG site, which suggest that high concentrations of ambient N_2O_5 measured during this short period may not contribute significantly to nitrate formation (Fig. S3). Overall, the simulated nitrate of base case without N_2O_5 constrained agreed well with the observation suggesting the robustness of the model simulations.

Gaussian error propagation was used to evaluate the model performance, as described in Lu et al. (2012). The uncertainties of various measurement parameters (VOCS, trace gases, meteorological parameters, etc.) ranged from 0 to 20%, and uncertainties of reaction rates are in the order of ~20% (Lu et al., 2012), while less than 10% uncertainty is derived from deposition velocity (Lou et al., 2010). Therefore, the uncertainty of simulated results in the base model is estimated to be around 50%.

https://doi.org/10.5194/acp-2021-730
Preprint. Discussion started: 21 October 2021

Atmospheric Chemistry and Physics Discussions

3 Results and discussion

3.1 Overview of nitrate concentrations during the campaign

The temporal variations of mass concentrations of the major chemical components in PM_1 are shown in Fig. 2. The mean concentration of PM_1 was 41.7±23.1 μg m^{-3} at the GIG site during the investigated period, which was comparable with that at the Heshan site (40.6 ±15.5 μg m^{-3}). The aerosol composition differed between sites, with inorganic ions (sulfate, nitrate, and ammonia) higher and organic matter lower at the GIG site compared to the Heshan site.

Although the mass concentrations at the two sites were comparable, the mass fraction of nitrate in PM_1 at the GIG site increased from 10% to 33% as the mass concentration of PM_1 increased from 20 to 130 μg m^{-3} (Fig. 3), while the fraction of nitrate increased from 10% to 20% at the Heshan site, suggesting that nitrate plays a more important role in the increase in PM_1 at the urban site than that at the suburban site. In addition, although the concentration of sulfate was higher than that of nitrate during most of the sampling periods, as PM_1 increased the mass concentration ratio of nitrate/sulfate increased from 0.5 to 2.0 at the GIG site and from 0.5 to 1.5 at the Heshan site. The higher ratios of nitrate/sulfate during the polluted periods implies that reducing nitrate may be essential for reducing the occurrence of PM pollution in southern China. The increasing contributions of nitrate to PM_1 in this study were similar with those observed in northern China during haze pollution (Yang et al., 2017;Fu et al., 2020;Wen et al., 2015;Liu et al., 2015), suggesting the significance of nitrate mitigation to further reduce mass concentrations of fine particles in China.

The diurnal patterns of mean nitrate, NH_3, NO_2 and HNO_3 concentrations observed at the GIG and Heshan sites are shown in Fig. 4. The highest nitrate concentration was observed in the morning at the GIG site and during nighttime at the Heshan site, suggesting differences in the processes that dominated the formation of nitrate at the two sites. At the GIG site, nitrate rapidly increased from 4:00 to 9:00, but the concentrations of NH_3 and HNO_3 increased slowly. The concentration of NO_2 exhibited a decreasing trend during the nitrate growth period. As gaseous HNO_3 is mainly produced by the reaction of OH and NO_2, the accumulation of nitrate after sunrise might largely be attributable to the downward transport from the residual layer to the ground. The diurnal variations in O_3 and NO_x measured at the GIG and Canton Tower sites are shown in Fig. 5. The ground-based observations at the Canton Tower showed similar

https://doi.org/10.5194/acp-2021-730
Preprint. Discussion started: 21 October 2021


Atmospheric Chemistry and Physics Discussions

variation patterns of O_3 and NO_x to the GIG site. However, the average concentration of O_3 at 488 m was 2.4 times higher than that at the ground site during nighttime, and the low nocturnal concentrations of NO (1.8 ± 0.2 ppb) at the 488 m site would enhance the production of NO_3 and N_2O_5 (Wang et al., 2018b;McDuffie et al., 2019). Therefore, heterogeneous uptake of N_2O_5 during nighttime may be active at 488 m at urban site, which will be further investigated in Section 3.3. At the Heshan site, nitrate increased sharply in the early nighttime (before midnight), which may be attributable to the shallow nocturnal boundary layer or the enhanced nocturnal N_2O_5 heterogeneous uptake reactions. Subsequently, there was a significant increase in nitrate from 7:00 to 9:00. The concentration of NH_3 showed variation pattern that was similar with that of nitrate and increased after 7:00, while the concentrations of HNO_3 and NO_2 showed a decreasing trend from 7:00 to 9:00. The different growth characteristics of nitrate and the variation patterns of precursors at the two sites may be related to different formation processes, which will be discussed in detail later.

In this study, the wind speeds in the investigated periods at the GIG and Heshan sites were generally below 2 m s^{-1} (Table S3), which suggests that regional transport may have limited contributions to the abundance of nitrate at the observation sites. Therefore, the discussion of the chemical formation process of nitrate in this study focuses on local production.

The molar ratios of $[NH_4^+]$ to the sum of $2\times[SO_4^{2-}]+[NO_3^-]$ are calculated (Fig. S5) to determine whether there was enough NH_4^+ to neutralize nitrate. The molar ratios were approximately 1.0 at both GIG and Heshan sites, suggesting the presence of sufficient ammonia to neutralize both nitrate and sulfate. Based on these discussions, we conclude that the nitrate production was mainly attributable to the production of HNO_3 and/or reactive heterogeneous uptake of N_2O_5, which will be discussed in the subsequent section.

3.2 Contributions of different pathways to nitrate formation

The temporal variations in simulated and observed nitrate concentrations at the GIG and Heshan sites are presented in Fig. 6; simulated and observed nitrate showed similar concentrations and variation patterns. The model performance was evaluated using the mean bias (MB), index of agreement (IOA), and correlation coefficient (*r*) (Table S4) (Liu et al., 2019;Lyu et al., 2017;Wang et al., 2019;Curci et al., 2015). The IOA was larger than 0.7 and r was larger than 0.5 at both sites, indicating good

https://doi.org/10.5194/acp-2021-730
Preprint. Discussion started: 21 October 2021


Atmospheric Chemistry and Physics Discussions

agreements between simulated and observed nitrate concentrations. The temporal variations in simulated N_2O_5 and $ClNO_2$ concentrations were comparable with the observations at the Heshan site as shown in Fig. S3 (c, d), but the simulated results at the GIG site from October 9 to 10 were significantly lower than the observations (Fig.S3 (a, b)). The abnormally high observed concentrations of N_2O_5 and $ClNO_2$ that lasted for short periods (10-30 minutes) at the GIG site may be caused by transported air masses from upwind regions without well-mixed with fresh urban NO emissions. Simulation of these near-instantaneous processes transported to the site using a box model is difficult, as box model is more suitable to simulate the well-mixed airmass with little transport effects. However, the simulated nitrate concentrations without observed N_2O_5 constrained was adequately comparable with the observations as shown in Fig. S2, implying the influence of the instantaneously high concentrations of N_2O_5 on nitrate formation was negligible at the GIG site.

Based on these simulation results, we calculated the daily-averaged contributions of the two different reaction pathways to the nitrate concentration - the daytime OH + NO_2 reaction and the nighttime uptake of N_2O_5 in the nocturnal boundary layer and in the residual layer. Since the nitrate produced in the residual layer is only gradually mixed to the surface as the boundary layer develops during the following morning, while the nitrate contributed to the boundary layer column concentration always included the uptake of N_2O_5 in the residual layer during the whole nighttime (Wang et al., 2018a;Womack et al., 2019). The calculation methods to determine contribution to the boundary layer column concentrations and to ground-level nitrate concentrations should be distinguished.

To calculate the contribution to the boundary layer column concentration, the integral of the N_2O_5 uptake reaction from both the nocturnal surface layer and the residual layer directly contribute to nitrate column concentrations layer during the whole nighttime, weighted as 0.4 and 0.6 based on their altitude fractions of the two layers, respectively. This calculation for the contributions to column concentration is the same as the methods presented by Wang et al. (2018a) and Womack et al. (2019). However, to quantify the contribution of nitrate produced from the residual layer to the ground nitrate concentration, one must account for the dynamic exchange between the residual layer and the surface-based boundary layer that develops during daytime. The integral time for this dynamic exchange was assumed from 6:00 to 10:00 in the morning.

https://doi.org/10.5194/acp-2021-730
Preprint. Discussion started: 21 October 2021


Atmospheric Chemistry and Physics Discussions

Detailed descriptions of the calculations are provided in Text S2 in Supplementary Materials. The calculation about partitioning process from OH and NO_2 reaction in the daytime was the same in the two methods mentioned above, which was the partition part of the integral of the OH and NO_2 reaction during the daytime.

The contributions of nitrate to the boundary layer column concentration (i.e. average from ground to 1000 m) are shown in Fig. 7a. The contribution from the N_2O_5 uptake reaction in the residual layer was 17.9 μg m^{-3} day^{-1} at the GIG site, which was much greater than the N_2O_5 uptake in the nocturnal boundary layer (0.4 μg m^{-3} day^{-1}). This is caused by the fresh NO surface emissions, which titrate the NO_3 radical and ozone in the nocturnal boundary layer. The contribution from nocturnal nitrate production in the boundary layer was comparable with the contribution from OH and NO_2 reaction (13.2 μg m^{-3} day^{-1}) during the daytime. In contrast to the GIG site, the contribution of N_2O_5 uptake from the nocturnal boundary layer (6.2 μg m^{-3} day^{-1}) was comparable with that in the residual layer (4.4 μg m^{-3} day^{-1}) at the Heshan site. The similar nitrate concentration and N_2O_5 production rate between the nocturnal boundary layer and residual layer in Fig.S7 (c, d) was due to smaller NO emissions at the Heshan site. The results demonstrate that nocturnal nitrate production plays an important role in nitrate production in the boundary layer, with nighttime contributions of 58% at the urban site and 35% at the suburban site.

The relative magnitudes of the contributions to the daily-averaged surface nitrate of nitrate differ somewhat from the contributions to the entire boundary layer. The contributions from the three major pathways to surface nitrate concentrations at the two sites are compared in Fig. 7b. At the GIG site the production of nitrate from the OH and NO_2 reaction and downward transport from the residual layer were 13.2 μg m^{-3} day^{-1} and 16.6 μg m^{-3} day^{-1}, contributing 43% and 53% of ground-level nitrate concentrations, with a minor contribution (1.1 μg m^{-3} day^{-1}) from N_2O_5 uptake in the nocturnal boundary layer. This is similar with the results in Fig.7a, implying a large nitrate contribution from N_2O_5 uptake in the residual layer, but not in the nocturnal boundary layer at the urban site.

However, at the suburban Heshan site (Fig.7b), downward transport from the residual layer made no contribution to the surface nitrate concentration, which was smaller than the contribution of nitrate from the residual layer in Fig. 7a. This is due to the similar N_2O_5 uptake rate between the nocturnal boundary layer and residual layer

https://doi.org/10.5194/acp-2021-730
Preprint. Discussion started: 21 October 2021


Atmospheric Chemistry and Physics Discussions

(see Fig. S7), inducing gradient negligible convection between the two layers as the result of small concentration gradient (Brown et al., 2003;Baasandorj et al., 2017;Prabhakar et al., 2017). The OH and NO_2 reaction (19.9 μg m^{-3} day^{-1}) and nocturnal N_2O_5 uptake (15.6 μg m^{-3} day^{-1}) were the major nitrate formation pathways, which contributed 56% and 44% to the total nitrate production, respectively. Therefore, the importance of residual layer contribution to the surface nitrate can vary significantly and should be comprehensively evaluated in different environments. In addition, the nitrate contributions to the surface concentrations and boundary layer column concentrations can also be different in different regions, which should be clarified and distinguished in future studies.

In summary, the N_2O_5 uptake reaction was active in the residual layer both at urban and suburban sites, but the downward transport from the residual layer was a significant contributor to surface nitrate at the urban site, but not at the suburban site. This is attributable to the titration of the NO_3 radical and ozone by fresh NO emissions during the stagnant boundary layer at the urban site, resulting in the large difference of nitrate production between the residual and nocturnal boundary layers. In contrast, at the suburban site, lower NO emissions favored NO_3 production and heterogeneous uptake of N_2O_5 both in the nocturnal boundary layer and the residual layer.

3.3 Control of NOx and VOCs as mitigation strategies of nitrate

Overall, the contributions of nitrate from the three major pathways, all involving NO_x and ozone, suggest that nitrate formation depends not only on the reactions of NO_x but also is closely associated with the VOCs-NO_x-O_3 chemistry. Therefore, the influence of both NO_x and VOCs reduction on nitrate production should be considered in formulating policies to control aerosol pollution.

In this study, we adopted the widely used EKMA approach, generally used for ozone sensitivity analysis (Edwards et al., 2014;Mazzuca et al., 2016;Xue et al., 2014b;Wang et al., 2015) to investigate the response of nitrate formation in changing emissions of VOCs and NO_x. The dependence of simulated nitrate concentrations with changing of VOCs and NO_x concentration allow to construct isopleths of nitrate and ozone production at the GIG and Heshan sites, as displayed in Fig. 8. The production of nitrate and ozone were in the VOCs-limited regime at the GIG site, and in the transition regime at the Heshan site. As shown in Fig. 9, an initial reduction of NO_x

https://doi.org/10.5194/acp-2021-730
Preprint. Discussion started: 21 October 2021


Atmospheric Chemistry and Physics Discussions

emissions would increase nitrate and ozone concentrations at the GIG site, but decrease those concentrations at the Heshan site. An initial decrease in VOCs concentrations would decrease nitrate and ozone concentrations at both sites. These results suggest that control of VOCs emissions will efficiently reduce nitrate and ozone production in both urban and suburban areas, but control of NO_x emissions will give different responses between urban and suburban area for both ozone and nitrate. Fig. 9 show that the nitrate sensitivity to the reduction of VOCs and NO_x emissions was identical to the response of ozone at both sites. These results demonstrate the possibility of synergetic control for nitrate and ozone at both urban and suburban sites through VOCs control.

The accuracy of the isopleth plots in Fig. 8 depends on several variables and parameters included in the box model. Figs S8–9 show the results of simulation experiments on the dependence of the isopleths upon changing various parameterization for estimating HONO concentrations and $ClNO_2$ yields as described in Text S3. The sensitivity of nitrate and ozone did not change, although the peak concentrations of ozone and nitrate did change, which supports the reliability of the results discussed above.

As nitrate and ozone exhibit similar sensitivity to the reduction of NO_x and VOCs, different VOCs/NO_x ratios may point to different control strategies. In the cases of the Heshan and GIG sites, the reduction of NO_x can adequately control nitrate production with a VOCs/NO_x ratio of 2.13 at the Heshan site, while a contrary result can be found at the GIG site (with a VOCs/NO_x ratio of 0.97) in the initial stage. The simulated results at the GIG site agree well with those reported in the urban areas of Shanghai in China (Dong et al., 2014) and the Salt Lake City and San Joaquin Valley in the US (Betty and Christian, 2001;Womack et al., 2019), which all emphasized the decrease of nitrate production with the reduction of VOCs emissions, and the enhanced nitrate production with NO_x reduction. The results at the Heshan site were consistent with the simulations at the suburban site of northern China, where a higher VOCs/NO_x ratio was found (Wen et al., 2018;Lu et al., 2019). The synergetic reduction of NO_x and VOCs is necessary to effectively mitigate the nitrate production in consideration of the different VOCs/NO_x ratios in the urban and suburban areas.

The above discussions revealed that direct reduction of NO_x may not lead to a decrease in nitrate production. Meanwhile, the reduction of VOCs is effective to mitigate nitrate production, though they were not the direct precursors of nitrate. To illustrate these findings, the impacts of changing VOCs and NO_x on the production rate

https://doi.org/10.5194/acp-2021-730
Preprint. Discussion started: 21 October 2021


Atmospheric Chemistry and Physics Discussions

of the OH radical, and the rate of OH plus NO_2, and the N_2O_5 uptake reaction were evaluated. During daytime nitrate production involves OH production and its subsequent reaction with NO_2. As shown in Fig. 10, the NO_x-saturated condition at the GIG site provided sufficient NO_2 to quench the OH radical during daytime. Initial reduction of NO_x will increase ozone production and thereby drive more production of OH, leading to increase in the OH and NO_2 reaction rates. When NO_x is lower than 30% of the base case emissions, ozone production would decrease and lead to the decrease of OH production and its reaction with NO_2, which in turn bring about a decrease in nitrate production. In contrast, at the Heshan site, the base case NO_x concentrations are lower, giving a production rate of OH that is already sensitive to both NO_x and VOCs reductions. The model results indicates that further emission reductions in both NO_x and VOCs will simultaneously mitigate the production of nitrate and ozone.

During nighttime, the decrease in NO_x will reduce the titration effect of NO on NO_3 radical and ozone at the GIG site, which enhances production of N_2O_5 and promotes nitrate production in both the nocturnal boundary layer and the residual layer (Fig. 11). However, at the Heshan site, the reduction of NO_x cuts down the sources of NO_2 and NO_3, decreasing the formation of N_2O_5 and thus its heterogeneous uptake to produce nitrate. The reduction of VOCs decreases ozone formation during daytime, thus attenuating the nocturnal formation of NO_3, N_2O_5 and nitrate at both the GIG and Heshan sites.

In summary, nitrate and ozone show similar responses to the reduction of NO_x and VOCs for both daytime and nighttime chemical processes, as the result of the coupling between the formation reactions of ozone and nitrate. The results of this study emphasize the complex effects of reductions of NO_x emissions on nitrate concentrations in the urban and suburban areas. In addition, the initial reduction of VOCs emissions would be effective in the concurrent mitigation of ozone and nitrate, suggesting that the reduction of VOCs at present is an effective method for the synergistic control of ozone and $PM_{2.5}$ at present. As there are limitations of box modeling, a comprehensive three-dimensional model assessment is needed on a regional scale.

4 Conclusions

In this study, we use an observation-constrained box model to explore the nitrate formation pathways and implications for nitrate mitigation strategies at urban and suburban sites. At both sites, the mass fraction of nitrate in PM_1 increased as the

https://doi.org/10.5194/acp-2021-730
Preprint. Discussion started: 21 October 2021


Atmospheric Chemistry and Physics Discussions

absolute PM_1 levels increased (from 10% to 33% at the urban site and from 10% to 20% at the suburban site), suggesting the important role played by nitrate in increasing particle concentrations in the PRD.

The model simulations demonstrate that chemical reactions in the daytime and at night both contributed significantly to formation of nitrate in the boundary layer at the two sites, with nighttime contributions of 58% at the urban site and 35% at the suburban site. However, nighttime reactions predominately occurred aloft in the residual layer at the urban site and downward transport from the residual layer in the morning are important source (53%) for surface nitrate at the urban site, whereas similar amounts of nitrate were produced in the nocturnal boundary layer and residual layer at the suburban site, which results in little downward transport of nitrate from the residual layer to the ground at this region. The spatial differences of nocturnal reactions and the opposite contributions from downward transport of the residual layer to surface nitrate at urban and suburban sites were attributed to different fresh emissions and concentration levels of NO_x at the two sites during the night time, suggesting that nitrate production under different NO_x conditions should be explored to better understand the its formation pathways.

The non-linear relationships between nitrate and NO_x, VOCs was developed to investigate the nitrate mitigation strategies. The simulations demonstrated that the formation processes of both nitrate and ozone were in the VOCs-limited region at the urban site and in the transition region at the suburban site. The same sensitivity regimes of nitrate and ozone at two sites was caused by the similar chemical processes that account to produce nitrate and ozone. These results suggest that control of VOCs emissions would effectively mitigate nitrate in both urban and suburban areas.

Overall, the formation processes of nitrate are systematically investigated in both urban and suburban areas in this study, which provides the opportunity to identify different influencing factors of nitrate production in different environments and offers insights into the comprehensive mitigation of nitrate pollution in regional scale. NO_x emission controls alone might not be an effective strategy for reducing the nitrate production, while the reduction of VOCs emissions would take effect in the concurrent mitigation of ozone and nitrate. Thus, an emission control policy focusing on VOCs will be an effective means for the synergistic control of ozone and $PM_{2.5}$ at present. In the long-term, multi-pollutant control should be implemented to achieve better control strategies for ozone and $PM_{2.5}$. Given the limitations of the box model, three-

https://doi.org/10.5194/acp-2021-730
Preprint. Discussion started: 21 October 2021


Atmospheric Chemistry and Physics Discussions

546 dimensional models should be used to further investigate the synergistic control of
547 ozone and particles on the regional scale.

548 Data availability

549 The observational data used in this study are available from corresponding authors
550 upon request (byuan@jnu.edu.cn)

551 Author contributions

552 BY and MS designed the research. SXY, YWP, SH, WC, WWH, CLP, CMW,
553 ZLW, TGL, EZ, MFC, XBL, SHW, CHW, WWJ, CSY, WS and PC contributed to data
554 collection. SXY performed the data analysis, with contributions from JZ，DD. Parrish,
555 XJH, CCL, XYY, YS, HCW, DHC, XMW, ZYZ, JYZ and XMW. SXY and BY
556 prepared the manuscript with contributions from the other authors. All the authors
557 reviewed the manuscript.

558 Competing interests

559 The authors declare that they have no known competing financial interests or personal
560 relationships that could have appeared to influence the work reported in this paper.

561 Acknowledgments

562 This work was supported by the National Key R&D Plan of China (grant No.
563 2019YFE0106300, 2018YFC0213904, 2016YFC0202206), the National Natural
564 Science Foundation of China (grant No. 41877302), the National Natural Science
565 Foundation of China (grant No. 41905111), Guangdong Natural Science Funds for
566 Distinguished Young Scholar (grant No. 2018B030306037), Key-Area Research and
567 Development Program of Guangdong Province (grant No. 2019B110206001),
568 Guangdong Soft Science Research Program (2019B101001005), and Guangdong
569 Innovative and Entrepreneurial Research Team Program (grant No. 2016ZT06N263).
570 This work was also supported by Special Fund Project for Science and Technology
571 Innovation Strategy of Guangdong Province (Grant No.2019B121205004).

572 References

573 Baasandorj, M., Hoch, S. W., Bares, R., Lin, J. C., Brown, S. S., Millet, D. B., Martin, R.,
574 Kelly, K., Zarzana, K. J., Whiteman, C. D., Dube, W. P., Tonnesen, G., Jaramillo, I. C., and

https://doi.org/10.5194/acp-2021-730
Preprint. Discussion started: 21 October 2021

575 Sohl, J.: Coupling between Chemical and Meteorological Processes under Persistent Cold-Air
576 Pool Conditions: Evolution of Wintertime PM2.5 Pollution Events and N2O5 Observations in
577 Utah's Salt Lake Valley, Environmental Science & Technology, 51, 5941-5950,
578 10.1021/acs.est.6b06603, 2017.
579 Bertram, T., and Thornton, J.: Toward a general parameterization of N 2 O 5 reactivity on
580 aqueous particles: The competing effects of particle liquid water, nitrate and chloride,
581 Atmospheric Chemistry and Physics Discussions, 9, 15181-15214, 2009.
582 Betty, P., and Christian: Sensitivity of particulate matter nitrate formation to precursor
583 emissions in the California San Joaquin Valley, Environmental Science & Technology, 35,
584 2979-2987, 2001.
585 Brown, S. S., Stark, H., Ryerson, T. B., Williams, E. J., Nicks Jr., D. K., Trainer, M.,
586 Fehsenfeld, F. C., and Ravishankara, A. R.: Nitrogen oxides in the nocturnal boundary layer:
587 Simultaneous in situ measurements of NO3, N2O5, NO2, NO, and O3, Journal of
588 Geophysical Research: Atmospheres, 108, 10.1029/2002jd002917, 2003.
589 Chen, W., Ye, Y., Hu, W., Zhou, H., Pan, T., Wang, Y., Song, W., Song, Q., Ye, C., Wang, C.,
590 Wang, B., Huang, S., Yuan, B., Zhu, M., Lian, X., Zhang, G., Bi, X., Jiang, F., Liu, J.,
591 Canonaco, F., Prevot, A. S. H., Shao, M., and Wang, X.: Real-time characterization of aerosol
592 compositions, sources and aging processes in Guangzhou during PRIDE-GBA 2018
593 campaign, Journal of Geophysical Research: Atmospheres, n/a, e2021JD035114,
594 https://doi.org/10.1029/2021JD035114, 2021.
595 Chen, X., Wang, H., Lu, K., Li, C., Zhai, T., Tan, Z., Ma, X., Yang, X., Liu, Y., Chen, S.,
596 Dong, H., Li, X., Wu, Z., Hu, M., Zeng, L., and Zhang, Y.: Field Determination of Nitrate
597 Formation Pathway in Winter Beijing, Environmental Science & Technology,
598 10.1021/acs.est.0c00972, 2020.
599 Curci, G., Ferrero, L., Tuccella, P., Barnaba, F., Angelini, F., Bolzacchini, E., Carbone, C., Der
600 Gon, H. A. C. D. V., Facchini, M. C., and Gobbi, G. P.: How much is particulate matter near
601 the ground influenced by upper-level processes within and above the PBL? A summertime
602 case study in Milan (Italy) evidences the distinctive role of nitrate, Atmospheric Chemistry
603 and Physics, 15, 2629-2649, 2015.
604 Dong, H. B., Zeng, L. M., Hu, M., Wu, Y. S., Zhang, Y. H., Slanina, J., Zheng, M., Wang, Z.
605 F., and Jansen, R.: Technical Note: The application of an improved gas and aerosol collector
606 for ambient air pollutants in China, Atmos. Chem. Phys., 12, 10519-10533, 10.5194/acp-12-
607 10519-2012, 2012.
608 Dong, X., Li, J., Fu, J. S., Gao, Y., Huang, K., and Zhuang, G.: Inorganic aerosols responses
609 to emission changes in Yangtze River Delta, China, Science of The Total Environment, 481,
610 522-532, 2014.
611 Edwards, P. M., Brown, S. S., Roberts, J. M., Ahmadov, R., Banta, R. M., deGouw, J. A.,

https://doi.org/10.5194/acp-2021-730
Preprint. Discussion started: 21 October 2021


Atmospheric Chemistry and Physics Discussions

612 Dubé, W. P., Field, R. A., Flynn, J. H., Gilman, J. B., Graus, M., Helmig, D., Koss, A.,
613 Langford, A. O., Lefer, B. L., Lerner, B. M., Li, R., Li, S.-M., McKeen, S. A., Murphy, S. M.,
614 Parrish, D. D., Senff, C. J., Soltis, J., Stutz, J., Sweeney, C., Thompson, C. R., Trainer, M. K.,
615 Tsai, C., Veres, P. R., Washenfelder, R. A., Warneke, C., Wild, R. J., Young, C. J., Yuan, B.,
616 and Zamora, R.: High winter ozone pollution from carbonyl photolysis in an oil and gas
617 basin, Nature, 514, 351, 10.1038/nature13767, 2014.
618 Ervens, B., George, C., Williams, J. E., Buxton, G. V., Salmon, G. A., Bydder, M., Wilkinson,
619 F., Dentener, F., Mirabel, P., Wolke, R., and Herrmann, H.: CAPRAM 2.4 (MODAC
620 mechanism): An extended and condensed tropospheric aqueous phase mechanism and its
621 application, Journal of Geophysical Research: Atmospheres, 108, 10.1029/2002JD002202,
622 2003.
623 Fu, X., Wang, T., Gao, J., Wang, P., Liu, Y., Wang, S., Zhao, B., and Xue, L.: Persistent Heavy
624 Winter Nitrate Pollution Driven by Increased Photochemical Oxidants in Northern China,
625 Environmental Science & Technology, 54, 3881-3889, 10.1021/acs.est.9b07248, 2020.
626 Gen, M., Zhang, R., Huang, D. D., Li, Y., and Chan, C. K.: Heterogeneous SO2 Oxidation in
627 Sulfate Formation by Photolysis of Particulate Nitrate, Environmental Science & Technology
628 Letters, 6, 86-91, 10.1021/acs.estlett.8b00681, 2019.
629 Geyer, A., and Stutz, J.: Vertical profiles of NO3, N2O5, O3, and NOx in the nocturnal
630 boundary layer: 2. Model studies on the altitude dependence of composition and chemistry,
631 Journal of Geophysical Research, 109, 2004.
632 Griffith, S. M., Huang, X. H. H., Louie, P. K. K., and Yu, J. Z.: Characterizing the
633 thermodynamic and chemical composition factors controlling PM2.5 nitrate: Insights gained
634 from two years of online measurements in Hong Kong, Atmospheric Environment, 122, 864-
635 875, https://doi.org/10.1016/j.atmosenv.2015.02.009, 2015.
636 Hou, X., Chan, C., Dong, G., and Yim, S.: Impacts of transboundary air pollution and local
637 emissions on PM2. 5 pollution in the Pearl River Delta region of China and the public health,
638 and the policy implications, Environmental Research Letters, 14, 034005, 2019.
639 Hu, W., Hu, M., Hu, W., Jimenez, J. L., Yuan, B., Chen, W., Wang, M., Wu, Y., Chen, C.,
640 Wang, Z., Peng, J., Zeng, L., and Shao, M.: Chemical composition, sources, and aging
641 process of submicron aerosols in Beijing: Contrast between summer and winter, Journal of
642 Geophysical Research: Atmospheres, 121, 1955-1977,
643 https://doi.org/10.1002/2015JD024020, 2016.
644 Jacob, D. J.: Heterogeneous chemistry and tropospheric ozone, Atmospheric Environment,
645 34, 2131-2159, https://doi.org/10.1016/S1352-2310(99)00462-8, 2000.
646 Li, H., Zhang, Q., Zheng, B., Chen, C., Wu, N., Guo, H., Zhang, Y., Zheng, Y., Li, X., and He,
647 K.: Nitrate-driven urban haze pollution during summertime over the North China Plain,
648 Atmos. Chem. Phys., 18, 5293-5306, 10.5194/acp-18-5293-2018, 2018.

https://doi.org/10.5194/acp-2021-730
Preprint. Discussion started: 21 October 2021


Atmospheric Chemistry and Physics Discussions

649 Li, L., Lu, C., Chan, P.-W., Zhang, X., Yang, H.-L., Lan, Z.-J., Zhang, W.-H., Liu, Y.-W., Pan,
650 L., and Zhang, L.: Tower observed vertical distribution of PM2.5, O3 and NOx in the Pearl
651 River Delta, Atmospheric Environment, 220, 117083,
652 https://doi.org/10.1016/j.atmosenv.2019.117083, 2020.
653 Li, S. M., Anlauf, K., and Wiebe, H.: Heterogeneous nighttime production and deposition of
654 particle nitrate at a rural site in North America during summer 1988, Journal of Geophysical
655 Research: Atmospheres, 98, 5139-5157, 1993.
656 Lin, Y. C., Zhang, Y. L., Fan, M. Y., and Bao, M.: Heterogeneous formation of particulate
657 nitrate under ammonium-rich regimes during the high-PM2.5 events in Nanjing, China,
658 Atmos. Chem. Phys., 20, 3999-4011, 10.5194/acp-20-3999-2020, 2020.
659 Liu, J., Ren, C., Huang, X., Nie, W., Wang, J., Sun, P., Chi, X., and Ding, A.: Increased
660 Aerosol Extinction Efficiency Hinders Visibility Improvement in Eastern China, Geophysical
661 Research Letters, 47, e2020GL090167, https://doi.org/10.1029/2020GL090167, 2020.
662 Liu, X., Sun, K., Qu, Y., Hu, M., Sun, Y., Zhang, F., and Zhang, Y.: Secondary formation of
663 sulfate and nitrate during a haze episode in megacity Beijing, China, Aerosol Air Qual. Res,
664 15, 2246-2257, 2015.
665 Liu, X., Lyu, X., Wang, Y., Jiang, F., and Guo, H.: Intercomparison of O3 formation and
666 radical chemistry in the past decade at a suburban site in Hong Kong, Atmos. Chem. Phys.,
667 19, 5127-5145, 10.5194/acp-19-5127-2019, 2019.
668 Lou, S., Holland, F., Rohrer, F., Lu, K., Bohn, B., Brauers, T., Chang, C., Fuchs, H., Häseler,
669 R., and Kita, K.: Atmospheric OH reactivities in the Pearl River Delta-China in summer 2006:
670 measurement and model results, Atmospheric Chemistry and Physics, 10, 11243, 2010.
671 Lu, K., Rohrer, F., Holland, F., Fuchs, H., Bohn, B., Brauers, T., Chang, C., Häseler, R., Hu,
672 M., and Kita, K.: Observation and modelling of OH and HO2 concentrations in the Pearl
673 River Delta 2006: a missing OH source in a VOC rich atmosphere, Atmospheric chemistry
674 and physics, 12, 1541, 2012.
675 Lu, K., Fuchs, H., Hofzumahaus, A., Tan, Z., Wang, H., Zhang, L., Schmitt, S. H., Rohrer, F.,
676 Bohn, B., Broch, S., Dong, H., Gkatzelis, G. I., Hohaus, T., Holland, F., Li, X., Liu, Y., Liu,
677 Y., Ma, X., Novelli, A., Schlag, P., Shao, M., Wu, Y., Wu, Z., Zeng, L., Hu, M., Kiendler-
678 Scharr, A., Wahner, A., and Zhang, Y.: Fast Photochemistry in Wintertime Haze:
679 Consequences for Pollution Mitigation Strategies, Environmental Science & Technology,
680 10.1021/acs.est.9b02422, 2019.
681 Lu, K. D., Hofzumahaus, A., Holland, F., Bohn, B., Brauers, T., Fuchs, H., Hu, M., seler, R.
682 H., Kita, K., Kondo, Y., Li, X., Lou, S. R., Oebel, A., Shao, M., Zeng, L. M., Wahner, A., Zhu,
683 T., Zhang, Y. H., and Rohrer, F.: Missing OH source in a suburban environment near Beijing:
684 observed and modelled OH and HO2 concentrations in summer 2006, Atmospheric Chemistry
685 and Physics (ACP) & Discussions (ACPD), 2013.

https://doi.org/10.5194/acp-2021-730
Preprint. Discussion started: 21 October 2021

686 Lyu, X., Wang, N., Guo, H., Xue, L., Jiang, F., Zeren, Y., Cheng, H., Cai, Z., Han, L., and
687 Zhou, Y.: Causes of a continuous summertime O3 pollution event in Jinan, a central city in the
688 North China Plain, Atmos. Chem. Phys., 19, 3025-3042, 10.5194/acp-19-3025-2019, 2019.
689 Lyu, X. P., Zeng, L. W., Guo, H., Simpson, I. J., Ling, Z. H., Wang, Y., Murray, F., Louie, P.
690 K. K., Saunders, S. M., Lam, S. H. M., and Blake, D. R.: Evaluation of the effectiveness of air
691 pollution control measures in Hong Kong, Environmental Pollution, 220, 87-94,
692 https://doi.org/10.1016/j.envpol.2016.09.025, 2017.
693 Mazzuca, G. M., Ren, X., Loughner, C. P., Estes, M., Crawford, J. H., Pickering, K. E.,
694 Weinheimer, A. J., and Dickerson, R. R.: Ozone production and its sensitivity to NOx and
695 VOCs: results from the DISCOVER-AQ field experiment, Houston 2013, Atmos. Chem.
696 Phys., 13, 14463-14474, 2016.
697 McDuffie, E. E., Fibiger, D. L., Dubé, W. P., Lopez-Hilfiker, F., Lee, B. H., Thornton, J. A.,
698 Shah, V., Jaeglé, L., Guo, H., Weber, R. J., Michael Reeves, J., Weinheimer, A. J., Schroder, J.
699 C., Campuzano-Jost, P., Jimenez, J. L., Dibb, J. E., Veres, P., Ebben, C., Sparks, T. L.,
700 Wooldridge, P. J., Cohen, R. C., Hornbrook, R. S., Apel, E. C., Campos, T., Hall, S. R.,
701 Ullmann, K., and Brown, S. S.: Heterogeneous N2O5 Uptake During Winter: Aircraft
702 Measurements During the 2015 WINTER Campaign and Critical Evaluation of Current
703 Parameterizations, Journal of Geophysical Research: Atmospheres, 123, 4345-4372,
704 10.1002/2018JD028336, 2018.
705 McDuffie, E. E., Womack, C. C., Fibiger, D. L., Dube, W. P., Franchin, A., Middlebrook, A.
706 M., Goldberger, L., Lee, B. H., Thornton, J. A., Moravek, A., Murphy, J. G., Baasandorj, M.,
707 and Brown, S. S.: On the contribution of nocturnal heterogeneous reactive nitrogen chemistry
708 to particulate matter formation during wintertime pollution events in Northern Utah, Atmos.
709 Chem. Phys., 19, 9287-9308, 10.5194/acp-19-9287-2019, 2019.
710 Mozurkewich, M.: The dissociation constant of ammonium nitrate and its dependence on
711 temperature, relative humidity and particle size, Atmospheric Environment. Part A. General
712 Topics, 27, 261-270, https://doi.org/10.1016/0960-1686(93)90356-4, 1993.
713 Pathak, R. K., Wu, W. S., and Wang, T.: Summertime PM_{2.5} ionic species in
714 four major cities of China: nitrate formation in an ammonia-deficient atmosphere, Atmos.
715 Chem. Phys., 9, 1711-1722, 10.5194/acp-9-1711-2009, 2009.
716 Pathak, R. K., Wang, T., and Wu, W. S.: Nighttime enhancement of PM2.5 nitrate in
717 ammonia-poor atmospheric conditions in Beijing and Shanghai: Plausible contributions of
718 heterogeneous hydrolysis of N2O5 and HNO3 partitioning, Atmospheric Environment, 45,
719 1183-1191, https://doi.org/10.1016/j.atmosenv.2010.09.003, 2011.
720 Prabhakar, G., Parworth, C. L., Zhang, X., Kim, H., Young, D. E., Beyersdorf, A. J., Ziemba,
721 L. D., Nowak, J. B., Bertram, T. H., Faloona, I. C., Zhang, Q., and Cappa, C. D.:
722 Observational assessment of the role of nocturnal residual-layer chemistry in determining

https://doi.org/10.5194/acp-2021-730
Preprint. Discussion started: 21 October 2021


Atmospheric Chemistry and Physics Discussions

723 daytime surface particulate nitrate concentrations, Atmos. Chem. Phys., 17, 14747-14770,
724 10.5194/acp-17-14747-2017, 2017.
725 Qin, Y. M., Tan, H. B., Li, Y. J., Schurman, M. I., Li, F., Canonaco, F., Prévôt, A. S. H., and
726 Chan, C. K.: Impacts of traffic emissions on atmospheric particulate nitrate and organics at a
727 downwind site on the periphery of Guangzhou, China, Atmos. Chem. Phys., 17, 10245-
728 10258, 10.5194/acp-17-10245-2017, 2017.
729 Riedel, T. P., Wolfe, G. M., Danas, K. T., Gilman, J. B., Kuster, W. C., Bon, D. M., Vlasenko,
730 A., Li, S. M., Williams, E. J., Lerner, B. M., Veres, P. R., Roberts, J. M., Holloway, J. S.,
731 Lefer, B., Brown, S. S., and Thornton, J. A.: An MCM modeling study of nitryl chloride
732 (ClNO₂) impacts on oxidation, ozone production and nitrogen oxide partitioning
733 in polluted continental outflow, Atmos. Chem. Phys., 14, 3789-3800, 10.5194/acp-14-3789-
734 2014, 2014.
735 Stelson, A. W., and Seinfeld, J. H.: Relative humidity and temperature dependence of the
736 ammonium nitrate dissociation constant, Atmospheric Environment (1967), 16, 983-992,
737 https://doi.org/10.1016/0004-6981(82)90184-6, 1982.
738 Su, T., Li, J., Tian, C., Zong, Z., Chen, D., and Zhang, G.: Source and formation of fine
739 particulate nitrate in South China: Constrained by isotopic modeling and online trace gas
740 analysis, Atmospheric Environment, 231, 117563,
741 https://doi.org/10.1016/j.atmosenv.2020.117563, 2020.
742 Tan, Z., Lu, K., Jiang, M., Su, R., Dong, H., Zeng, L., Xie, S., Tan, Q., and Zhang, Y.:
743 Exploring ozone pollution in Chengdu, southwestern China: A case study from radical
744 chemistry to O3-VOC-NOx sensitivity, Science of The Total Environment, 636, 775-786,
745 https://doi.org/10.1016/j.scitotenv.2018.04.286, 2018.
746 Tang, G., Wang, Y., Liu, Y., Wu, S., Huang, X., Yang, Y., Wang, Y., Ma, J., Bao, X., Liu, Z., Ji,
747 D., Li, T., Li, X., and Wang, Y.: Low particulate nitrate in the residual layer in autumn over
748 the North China Plain, Science of The Total Environment, 782, 146845,
749 https://doi.org/10.1016/j.scitotenv.2021.146845, 2021.
750 Tao, J., Zhang, Z., Tan, H., Zhang, L., Wu, Y., Sun, J., Che, H., Cao, J., Cheng, P., Chen, L.,
751 and Zhang, R.: Observational evidence of cloud processes contributing to daytime elevated
752 nitrate in an urban atmosphere, Atmospheric Environment, 186, 209-215,
753 https://doi.org/10.1016/j.atmosenv.2018.05.040, 2018.
754 Tao, Y., Ye, X., Ma, Z., Xie, Y., Wang, R., Chen, J., Yang, X., and Jiang, S.: Insights into
755 different nitrate formation mechanisms from seasonal variations of secondary inorganic
756 aerosols in Shanghai, Atmospheric Environment, 145, 1-9,
757 https://doi.org/10.1016/j.atmosenv.2016.09.012, 2016.
758 Wang, C., Yuan, B., Wu, C., Wang, S., Qi, J., Wang, B., Wang, Z., Hu, W., Chen, W., Ye, C.,
759 Wang, W., Sun, Y., Wang, C., Huang, S., Song, W., Wang, X., Yang, S., Zhang, S., Xu, W.,

https://doi.org/10.5194/acp-2021-730
Preprint. Discussion started: 21 October 2021

Atmospheric Chemistry and Physics Discussions

760 Ma, N., Zhang, Z., Jiang, B., Su, H., Cheng, Y., Wang, X., and Shao, M.: Measurements of
761 higher alkanes using NO+ chemical ionization in PTR-ToF-MS: important contributions of
762 higher alkanes to secondary organic aerosols in China, Atmos. Chem. Phys., 20, 14123-
763 14138, 10.5194/acp-20-14123-2020, 2020a.
764 Wang, H., Lu, K., Chen, X., Zhu, Q., Chen, Q., Guo, S., Jiang, M., Li, X., Shang, D., Tan, Z.,
765 Wu, Y., Wu, Z., Zou, Q., Zheng, Y., Zeng, L., Zhu, T., Hu, M., and Zhang, Y.: High N2O5
766 Concentrations Observed in Urban Beijing: Implications of a Large Nitrate Formation
767 Pathway, Environmental Science & Technology Letters, 4, 416-420,
768 10.1021/acs.estlett.7b00341, 2017a.
769 Wang, H., Lu, K., Tan, Z., Sun, K., Li, X., Hu, M., Shao, M., Zeng, L., Zhu, T., and Zhang, Y.:
770 Model simulation of NO3, N2O5 and ClNO2 at a rural site in Beijing during CAREBeijing-
771 2006, Atmospheric Research, 196, 97-107, https://doi.org/10.1016/j.atmosres.2017.06.013,
772 2017b.
773 Wang, H., Lu, K., Chen, X., Zhu, Q., Wu, Z., Wu, Y., and Sun, K.: Fast particulate nitrate
774 formation via N2O5 uptake aloft in winter in Beijing, Atmos. Chem. Phys., 18, 10483-10495,
775 10.5194/acp-18-10483-2018, 2018a.
776 Wang, H., Lu, K., Guo, S., Wu, Z., Shang, D., Tan, Z., Wang, Y., Le Breton, M., Lou, S.,
777 Tang, M., Wu, Y., Zhu, W., Zheng, J., Zeng, L., Hallquist, M., Hu, M., and Zhang, Y.:
778 Efficient N2O5 uptake and NO3 oxidation in the outflow of urban Beijing, Atmos. Chem.
779 Phys., 18, 9705-9721, 10.5194/acp-18-9705-2018, 2018b.
780 Wang, N., Guo, H., Jiang, F., Ling, Z. H., and Wang, T.: Simulation of ozone formation at
781 different elevations in mountainous area of Hong Kong using WRF-CMAQ model, Science of
782 The Total Environment, 505, 939-951, https://doi.org/10.1016/j.scitotenv.2014.10.070, 2015.
783 Wang, N., Lyu, X., Deng, X., Huang, X., Jiang, F., and Ding, A.: Aggravating O3 pollution
784 due to NOx emission control in eastern China, Science of The Total Environment, 677, 732-
785 744, https://doi.org/10.1016/j.scitotenv.2019.04.388, 2019.
786 Wang, Y., Zhang, Y., Hao, J., and Luo, M.: Seasonal and spatial variability of surface ozone
787 over China: contributions from background and domestic pollution, Atmos. Chem. Phys., 11,
788 3511-3525, 10.5194/acp-11-3511-2011, 2011.
789 Wang, Z., Yuan, B., Ye, C., Roberts, J., Wisthaler, A., Lin, Y., Li, T., Wu, C., Peng, Y., Wang,
790 C., Wang, S., Yang, S., Wang, B., Qi, J., Wang, C., Song, W., Hu, W., Wang, X., Xu, W., Ma,
791 N., Kuang, Y., Tao, J., Zhang, Z., Su, H., Cheng, Y., Wang, X., and Shao, M.: High
792 Concentrations of Atmospheric Isocyanic Acid (HNCO) Produced from Secondary Sources in
793 China, Environmental Science & Technology, 54, 11818-11826, 10.1021/acs.est.0c02843,
794 2020b.
795 Watson, J. G.: Visibility: Science and Regulation, Journal of The Air & Waste Management
796 Association, 52, 973-999, 2002.

https://doi.org/10.5194/acp-2021-730
Preprint. Discussion started: 21 October 2021

797 Wen, L., Chen, J., Yang, L., Wang, X., Caihong, X., Sui, X., Yao, L., Zhu, Y., Zhang, J., Zhu,
798 T., and Wang, W.: Enhanced formation of fine particulate nitrate at a rural site on the North
799 China Plain in summer: The important roles of ammonia and ozone, Atmospheric
800 Environment, 101, 294-302, https://doi.org/10.1016/j.atmosenv.2014.11.037, 2015.
801 Wen, L., Xue, L., Wang, X., Xu, C., Chen, T., Yang, L., Wang, T., Zhang, Q., and Wang, W.:
802 Summertime fine particulate nitrate pollution in the North China Plain: increasing trends,
803 formation mechanisms and implications for control policy, Atmos. Chem. Phys., 18, 11261-
804 11275, 10.5194/acp-18-11261-2018, 2018.
805 Wolfe, G. M., Marvin, M. R., Roberts, S. J., Travis, K. R., and Liao, J.: The Framework for 0-
806 D Atmospheric Modeling (F0AM) v3.1, Geosci. Model Dev., 9, 3309-3319, 10.5194/gmd-9-
807 3309-2016, 2016.
808 Womack, C. C., McDuffie, E. E., Edwards, P. M., Bares, R., de Gouw, J. A., Docherty, K. S.,
809 Dube, W. P., Fibiger, D. L., Franchin, A., Gilman, J. B., Goldberger, L., Lee, B. H., Lin, J. C.,
810 Long, R., Middlebrook, A. M., Millet, D. B., Moravek, A., Murphy, J. G., Quinn, P. K.,
811 Riedel, T. P., Roberts, J. M., Thornton, J. A., Valin, L. C., Veres, P. R., Whitehill, A. R., Wild,
812 R. J., Warneke, C., Yuan, B., Baasandorj, M., and Brown, S. S.: An odd oxygen framework
813 for wintertime ammonium nitrate aerosol pollution in urban areas: NOx and VOC control as
814 mitigation strategies, Geophysical Research Letters, 0, 10.1029/2019gl082028, 2019.
815 Wu, C., Wang, C., Wang, S., Wang, W., Yuan, B., Qi, J., Wang, B., Wang, H., Wang, C., Song,
816 W., Wang, X., Hu, W., Lou, S., Ye, C., Peng, Y., Wang, Z., Huangfu, Y., Xie, Y., Zhu, M.,
817 Zheng, J., Wang, X., Jiang, B., Zhang, Z., and Shao, M.: Measurement report: Important
818 contributions of oxygenated compounds to emissions and chemistry of volatile organic
819 compounds in urban air, Atmos. Chem. Phys., 20, 14769-14785, 10.5194/acp-20-14769-2020,
820 2020.
821 Xu, L., and Penner, J. E.: Global simulations of nitrate and ammonium aerosols and their
822 radiative effects, Atmos. Chem. Phys., 12, 9479-9504, 10.5194/acp-12-9479-2012, 2012.
823 Xue, J., Yuan, Z., Lau, A. K. H., and Yu, J. Z.: Insights into factors affecting nitrate in PM2.5
824 in a polluted high NOx environment through hourly observations and size distribution
825 measurements, Journal of Geophysical Research: Atmospheres, 119, 4888-4902,
826 10.1002/2013JD021108, 2014a.
827 Xue, L. K., Wang, T., Gao, J., Ding, A. J., Zhou, X. H., Blake, D. R., Wang, X. F., Saunders,
828 S. M., Fan, S. J., Zuo, H. C., Zhang, Q. Z., and Wang, W. X.: Ground-level ozone in four
829 Chinese cities: precursors, regional transport and heterogeneous processes, Atmos. Chem.
830 Phys., 14, 13175-13188, 10.5194/acp-14-13175-2014, 2014b.
831 Yang, Q., Su, H., Li, X., Cheng, Y., Lu, K., Cheng, P., Gu, J., Guo, S., Hu, M., and Zeng, L.:
832 Daytime HONO formation in the suburban area of the megacity Beijing, China, Science
833 China Chemistry, 57, 1032-1042, 2014.

https://doi.org/10.5194/acp-2021-730
Preprint. Discussion started: 21 October 2021

834 Yang, T., Sun, Y., Zhang, W., Wang, Z., Liu, X., Fu, P., and Wang, X.: Evolutionary processes
835 and sources of high-nitrate haze episodes over Beijing, Spring, Journal of Environmental
836 Sciences, 54, 142-151, https://doi.org/10.1016/j.jes.2016.04.024, 2017.
837 Ye, C., Gao, H., Zhang, N., and Zhou, X.: Photolysis of Nitric Acid and Nitrate on Natural
838 and Artificial Surfaces, Environmental Science & Technology, 50, 3530-3536,
839 10.1021/acs.est.5b05032, 2016.
840 Ye, C., Zhang, N., Gao, H., and Zhou, X.: Photolysis of Particulate Nitrate as a Source of
841 HONO and NOx, Environmental Science & Technology, 51, 6849-6856,
842 10.1021/acs.est.7b00387, 2017.
843 Ye, C., Yuan, B., Lin, Y., Wang, Z., Hu, W., Li, T., Chen, W., Wu, C., Wang, C., and Huang,
844 S.: Chemical characterization of oxygenated organic compounds in the gas phase and particle
845 phase using iodide CIMS with FIGAERO in urban air, Atmospheric Chemistry and Physics,
846 21, 8455-8478, 2021.
847 Yu, C., Wang, Z., Xia, M., Fu, X., Wang, W., Tham, Y. J., Chen, T., Zheng, P., Li, H., Shan, Y.,
848 Wang, X., Xue, L., Zhou, Y., Yue, D., Ou, Y., Gao, J., Lu, K., Brown, S. S., Zhang, Y., and
849 Wang, T.: Heterogeneous N2O5 reactions on atmospheric aerosols at four Chinese sites:
850 improving model representation of uptake parameters, Atmos. Chem. Phys., 20, 4367-4378,
851 10.5194/acp-20-4367-2020, 2020.
852 Yu, Y., Cheng, P., Li, H., Yang, W., Han, B., Song, W., Hu, W., Wang, X., Yuan, B., Shao, M.,
853 Huang, Z., Li, Z., Zheng, J., Wang, H., and Yu, X.: Budget of nitrous acid (HONO) and its
854 impacts on atmospheric oxidation capacity at an urban site in the fall season of Guangzhou,
855 China, Atmos. Chem. Phys. Discuss., 2021, 1-38, 10.5194/acp-2021-178, 2021.
856 Yuan, B., Chen, W., Shao, M., Wang, M., Lu, S., Wang, B., Liu, Y., Chang, C., and Wang, B.:
857 Measurements of ambient hydrocarbons and carbonyls in the Pearl River Delta (PRD), China,
858 Atmospheric Research, 116, 93-104, 2012.
859 Yuan, B., Liggio, J., Wentzell, J., Li, S. M., Stark, H., Roberts, J. M., Gilman, J., Lerner, B.,
860 Warneke, C., Li, R., Leithead, A., Osthoff, H. D., Wild, R., Brown, S. S., and de Gouw, J. A.:
861 Secondary formation of nitrated phenols: insights from observations during the Uintah Basin
862 Winter Ozone Study (UBWOS) 2014, Atmos. Chem. Phys., 16, 2139-2153, 10.5194/acp-16-
863 2139-2016, 2016.
864 Yun, H., Wang, T., Wang, W., Tham, Y. J., Li, Q., Wang, Z., and Poon, S. C. N.: Nighttime
865 NOx loss and ClNO2 formation in the residual layer of a polluted region: Insights from field
866 measurements and an iterative box model, Science of The Total Environment, 622-623, 727-
867 734, https://doi.org/10.1016/j.scitotenv.2017.11.352, 2018a.
868 Yun, H., Wang, W., Wang, T., Xia, M., Yu, C., Wang, Z., Poon, S. C. N., Yue, D., and Zhou,
869 Y.: Nitrate formation from heterogeneous uptake of dinitrogen pentoxide during a severe
870 winter haze in southern China, Atmos. Chem. Phys., 18, 17515-17527, 10.5194/acp-18-

https://doi.org/10.5194/acp-2021-730
Preprint. Discussion started: 21 October 2021

Atmospheric Chemistry and Physics Discussions

871 17515-2018, 2018b.
872 Zhang, H., An, Q., Zhao, S., Xie, B., and Liu, Q.: Advances in the research of optical
873 properties and radiative forcing of nitrate aerosols, Acta Meteorologica Sinica, 75, 539-551,
874 2017.
875 Zhang, R., Gen, M., Huang, D., Li, Y., and Chan, C. K.: Enhanced Sulfate Production by
876 Nitrate Photolysis in the Presence of Halide Ions in Atmospheric Particles, Environmental
877 Science & Technology, 54, 3831-3839, 10.1021/acs.est.9b06445, 2020.
878

https://doi.org/10.5194/acp-2021-730
Preprint. Discussion started: 21 October 2021

Atmospheric Chemistry and Physics Discussions

879

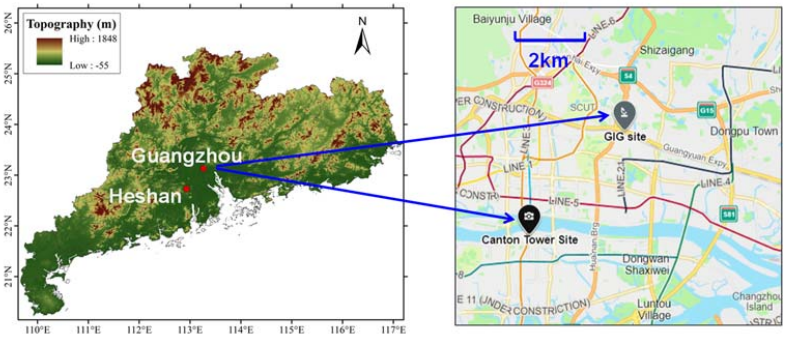

880

881 **Figure 1.** Sampling site at Guangzhou Institute of Geochemistry, Chinese Academy of
882 Sciences (GIG), Heshan and Canton Tower. Note that the map is extracted from
883 © Microsoft Bing maps by the authors.

884

https://doi.org/10.5194/acp-2021-730
Preprint. Discussion started: 21 October 2021

Atmospheric Chemistry and Physics Discussions

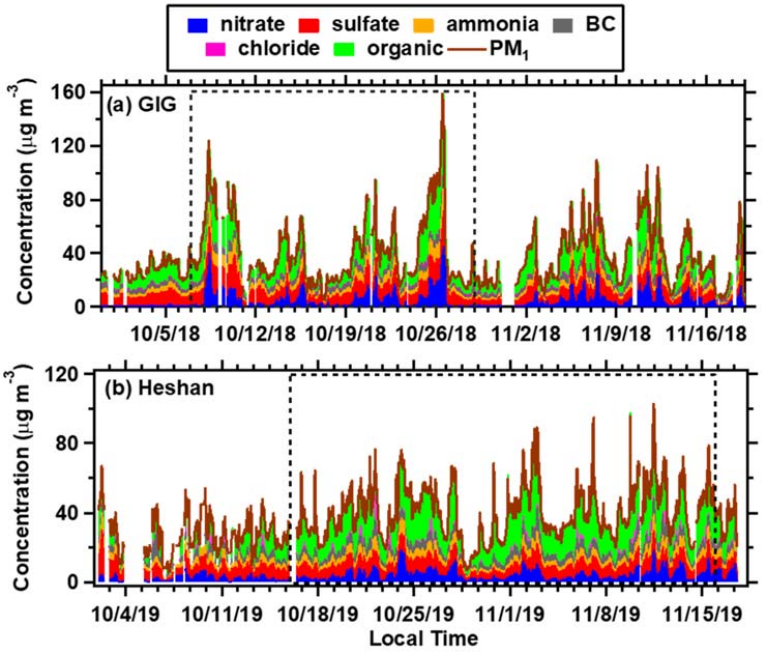

885

886 **Figure 2.** Temporal variations of the mass concentration of the major chemical
887 components in PM_1 including nitrate (NO_3^-), sulfate (SO_4^{2-}), ammonium (NH_4^+), black
888 carbon (BC), chloride (Cl^-) and organics at (a) GIG site and (b) Heshan site. The black
889 dashed rectangle represents the investigated period which had complete set of data.
890

https://doi.org/10.5194/acp-2021-730
Preprint. Discussion started: 21 October 2021

Atmospheric Chemistry and Physics Discussions

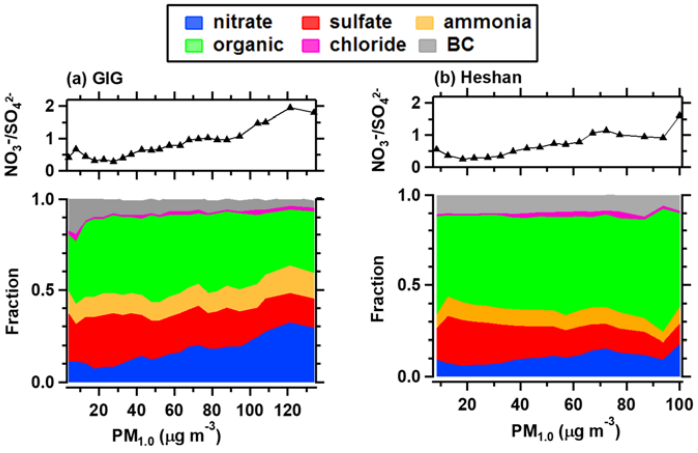

891

892 **Figure 3.** The mass concentration ratio of NO_3^-/SO_4^{2-} (top) and fractions of major
893 chemical components (bottom) in PM_1 at (a) GIG site and (b) Heshan site.
894

https://doi.org/10.5194/acp-2021-730
Preprint. Discussion started: 21 October 2021

Atmospheric Chemistry and Physics Discussions

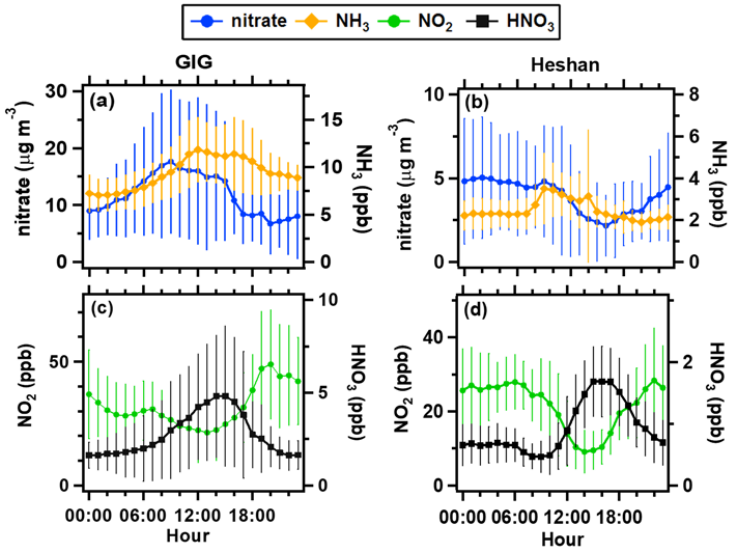

Figure 4. Diurnal variations of mean concentrations of nitrate and related pollution species at (a) GIG site and (b) Heshan site. The error bars represent the standard deviation of the means.

https://doi.org/10.5194/acp-2021-730
Preprint. Discussion started: 21 October 2021

Atmospheric Chemistry and Physics Discussions

900

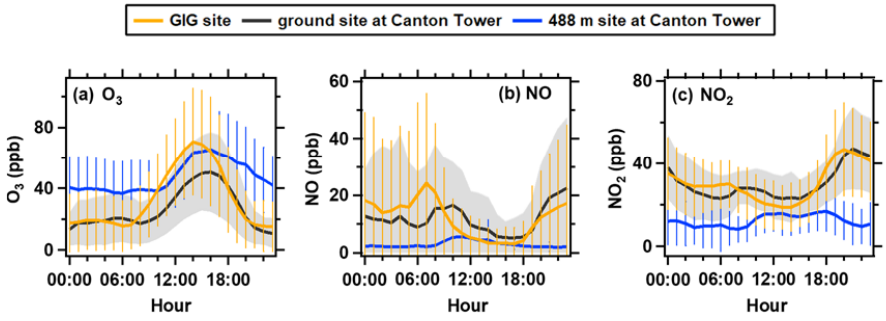

901

902 **Figure 5.** Diurnal variation of mean concentrations of (a) O_3, (b) NO, (c) NO_2 at GIG
903 (orange lines), and the ground and 488m sites of Canton Tower (black and blue lines,
904 respectively). The orange and blue error bars represent the standard deviations of the
905 mean concentrations at the GIG site and the 488m site of Canton Tower, the grey areas
906 show one standard deviation of the mean concentration at ground site of Canton Tower.

https://doi.org/10.5194/acp-2021-730
Preprint. Discussion started: 21 October 2021

Atmospheric Chemistry and Physics Discussions

907

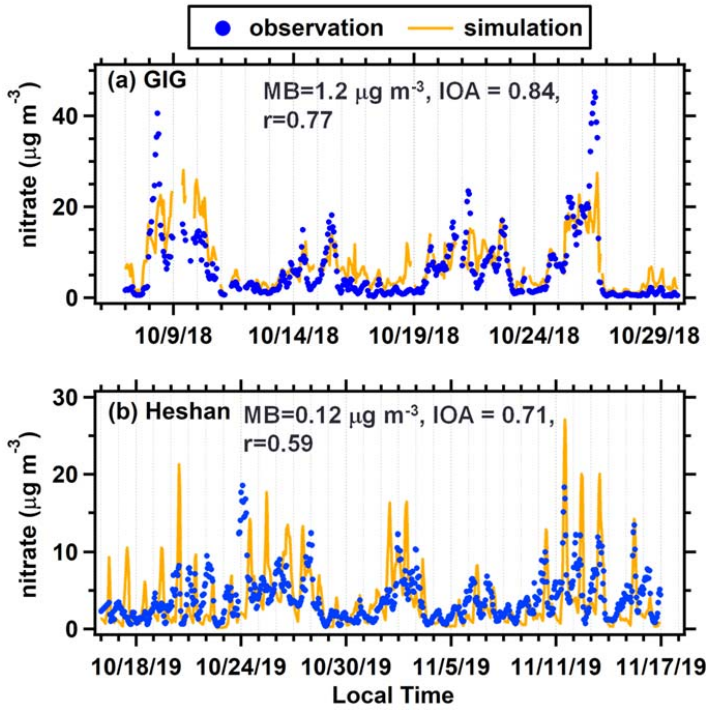

908

909 **Figure 6.** Comparison of the temporal simulated and observed nitrate at the (a) GIG
910 site and (b) Heshan site.

911

https://doi.org/10.5194/acp-2021-730
Preprint. Discussion started: 21 October 2021

Atmospheric Chemistry and Physics Discussions

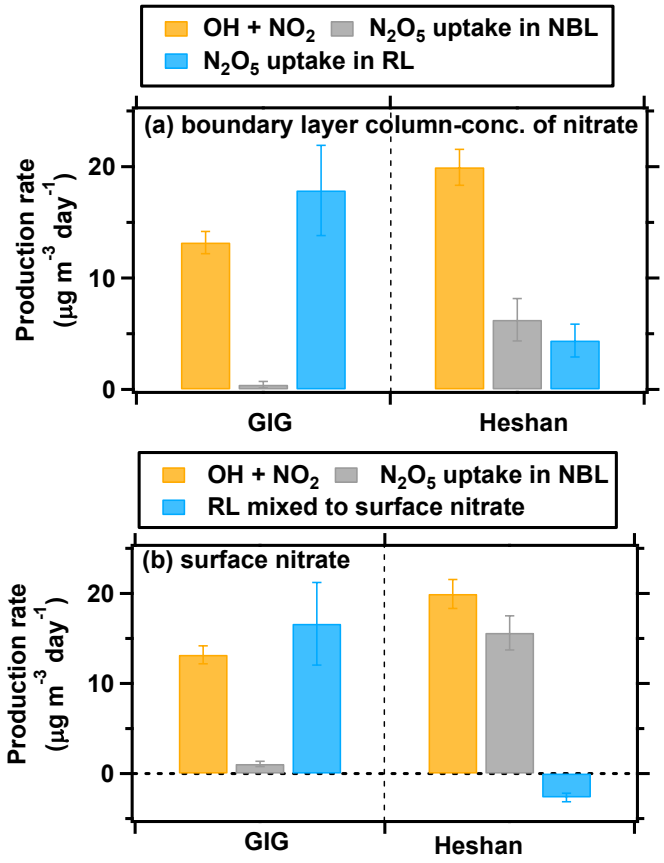

912

913 **Figure 7.** The daily-averaged contribution (a) to boundary layer column concentration
914 and (b) to surface nitrate from three pathways (OH +NO_2 reaction, N_2O_5 uptake in NBL,
915 and N_2O_5 uptake in RL/N_2O_5 uptake from RL mixed process) at the GIG and Heshan
916 sites. The error bars represent the standard deviations of the mean production rate.

917

https://doi.org/10.5194/acp-2021-730
Preprint. Discussion started: 21 October 2021

Atmospheric Chemistry and Physics Discussions

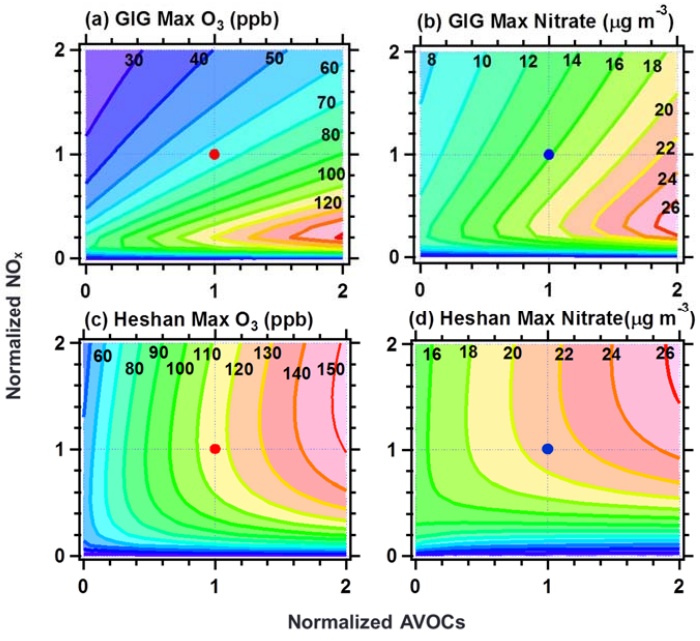

Figure 8. The simulated isopleths of ozone and nitrate with normalized NO_x and AVOCs concentration at the (a, b) GIG site and (c, d) Heshan site, each isopleth represents the maximum ozone and nitrate in the simulation, and the red and blue circles represent the base cases.

https://doi.org/10.5194/acp-2021-730
Preprint. Discussion started: 21 October 2021

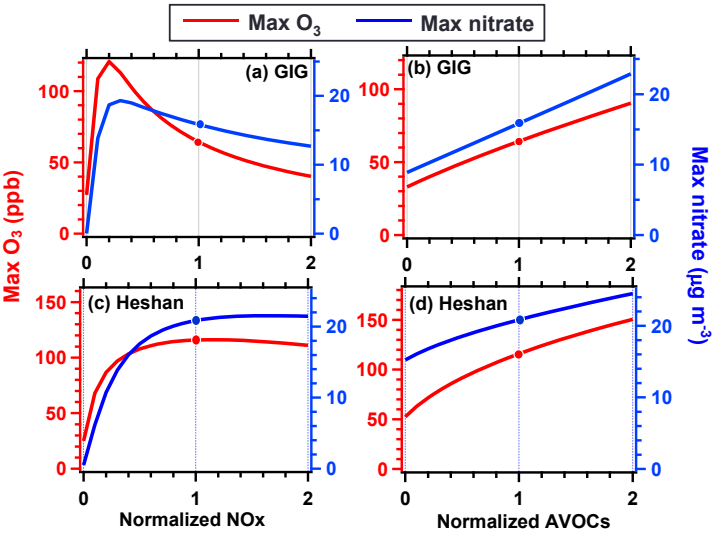

925

926 **Figure 9.** Simulated maximum ozone and nitrate concentration with normalized NOx
927 and AVOCs at the (a, b) GIG site and (c, d) Heshan site, cutting through the simulated
928 isopleth in Figure 8 with normalized AVOCs and NOx ratio at 1, respectively. The red
929 and blue circles represent the base cases.
930

https://doi.org/10.5194/acp-2021-730
Preprint. Discussion started: 21 October 2021

Atmospheric Chemistry and Physics Discussions

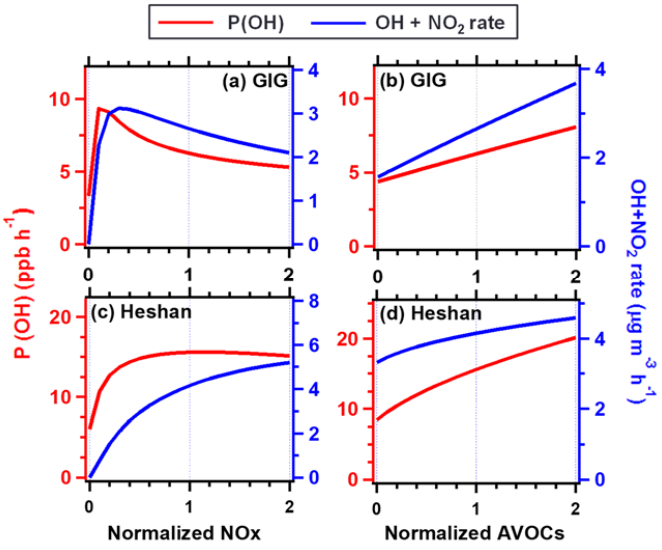

931

932 **Figure 10.** Simulated average production rates of OH (P (OH)) and the reaction rate of
933 OH and NO_2 with the normalized changes of NO_x and AVOCs emissions at the (a, b)
934 GIG site and (c, d) Heshan site.

935

https://doi.org/10.5194/acp-2021-730
Preprint. Discussion started: 21 October 2021

Atmospheric Chemistry and Physics Discussions

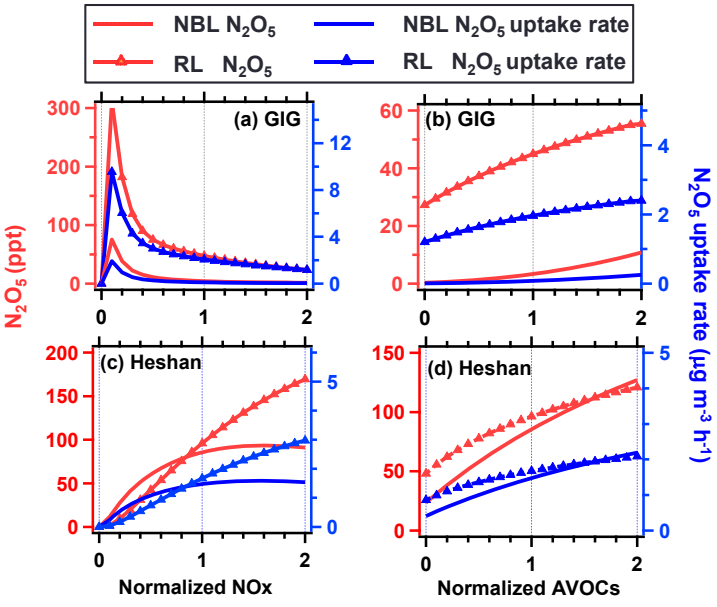

936

937 **Figure 11.** Simulated average concentration of N_2O_5 and production rate of N_2O_5
938 uptake with the normalized changes of NO_x and AVOCs emissions at the (a, b) GIG
939 site and (c, d) Heshan site in the NBL and RL.
940